



# RESEARCH ACTIVITIES

## Photo-Molecular Science

We study the interaction of atoms and molecules with optical fields with its possible applications to active control of atomic and molecular functionality and reactivity. We also develop novel light sources to promote those studies. Two research facilities, the Laser Research Center for Molecular Science and the UVSOR, closely collaborate with the Department.

The core topics of the Department include ultrahigh-precision coherent control of gas- and condensed-phase atoms and molecules, high-resolution optical microscopy applied to nanomaterials, synchrotron-based spectroscopy of core-excited molecules and solid-state materials, vacuum-UV photochemistry, and the development of novel laser- and synchrotron-radiation sources.

# Development of Advanced Near-Field Spectroscopic Imaging and Application to Nanomaterials

## Department of Photo-Molecular Science Division of Photo-Molecular Science I



**OKAMOTO, Hiromi**  
Professor  
[aho@ims.ac.jp]

### Education

1983 B.S. The University of Tokyo  
1991 Ph.D. The University of Tokyo

### Professional Employment

1985 Research Associate, Institute for Molecular Science  
1990 Research Associate, The University of Tokyo  
1993 Associate Professor, The University of Tokyo  
2000 Professor, Institute for Molecular Science  
Professor, The Graduate University for Advanced Studies

### Award

2012 The Chemical Society of Japan (CSJ) Award for Creative Work

### Member

Assistant Professor  
NARUSHIMA, Tetsuya  
IMS Research Assistant Professor  
NISHIYAMA, Yoshio  
Post-Doctoral Fellow  
KOWAKA, Yasuyuki  
Visiting Scientist  
SAIN, Basudeb\*  
JACK, Calum†  
Graduate Student  
HASHIYADA, Shun  
Technical Fellow  
ISHIKAWA, Akiko  
Secretary  
NOMURA, Emiko

**Keywords** Near-Field Optical Microscopy, Plasmons, Excited States of Nanomaterials

There is much demand for the studies of local optical properties of molecular assemblies and materials, to understand nanoscale physical and chemical phenomena and/or to construct nanoscale optoelectronic devices. Scanning near-field optical microscopy (SNOM) is an imaging method that enables spatial resolution beyond the diffraction limit of light. Combination of this technique with various advanced spectroscopic methods may provide direct methods to probe dynamics in nanomaterials and nanoscale functionalities. It may yield essential and basic knowledge to analyze origins of characteristic features of the nanomaterial systems. We have constructed apparatuses of near-field spectroscopy and microscopy for excited-state studies of nanomaterials, with the feasibilities of nonlinear and time-resolved measurements. The developed apparatuses enable near-field measurements of two-photon induced emission, femtosecond time-resolved signals, and circular dichroism, in addition to conventional transmission, emission, and Raman-scattering. Based on these methods, we are investigating the characteristic spatiotemporal behavior of various metal-nanostructure systems and molecu-

lar assemblies. Typical examples are shown in Figure 1. We succeeded in visualizing wave functions of resonant plasmon modes in single noble metal nanoparticles, confined optical fields in noble metal nanoparticle assemblies, and so forth.

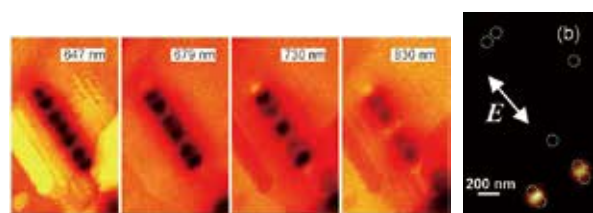


**Figure 1.** (Left four panels) Near-field transmission images of gold nanorod ( $20 \text{ nm}^D \times 510 \text{ nm}^L$ ). The wavelengths of observation were 647, 679, 730, and 830 nm from left to right. The spatial oscillating features were attributed to the square amplitudes of the resonant plasmonic wave functions. (Right) Near-field two-photon excitation image of dimers of spheric gold nanoparticles (diameter 100 nm) observed at 785 nm. The arrows indicates the incident light polarization. Dotted circles represent approximate positions of the particles.

### Selected Publications

- H. Okamoto, T. Narushima, Y. Nishiyama and K. Imura, "Local Optical Responses of Plasmon Resonance Visualized by Near-Field Optical Imaging," *Phys. Chem. Chem. Phys.* **17**, 6192–6206 (2015).
- H. Okamoto and K. Imura, "Visualizing the Optical Field Structures in Metal Nanostructures," *J. Phys. Chem. Lett.* **4**, 2230–2241 (2013).
- H. Okamoto and K. Imura, "Near-Field Optical Imaging of Enhanced Electric Fields and Plasmon Waves in Metal Nanostructures," *Prog. Surf. Sci.* **84**, 199–229 (2009).

## 1. Local Optical Activity in Achiral Two-Dimensional Gold Nanostructures<sup>1,2)</sup>

Since the discovery of molecular chirality, the geometrical chirality of a material, which means that the material has a non-superposable mirror image, has been considered the prerequisite for exhibiting optical activity of the structural origin. Circular dichroism (CD, defined as the differential absorption of left and right circularly polarized light) is a representative measurement method of optical activity. We recently developed a scanning near-field CD microscope, which is capable of optical imaging with CD of a specimen as the signal with a spatial resolution beyond the diffraction limit of light, and applied the method to local optical activity measurements of plasmonic chiral nanostructures. In the present study, we report an experimental demonstration of nanoscale local CD activities for highly symmetric achiral (non-chiral) rectangular gold nanostructures.<sup>1)</sup> Macroscopic CD spectral measurements of the nanostructure sample did not show any CD activity over the entire range of measured wavelengths, as expected from the achiral shape of the rectangle. In contrast, we found both locally positive and negative CD signals in a single rectangular nanostructure, whose spatial distribution was symmetric about the center of the rectangle, with strong CD signals at the corners (Figure 2(b)). The strong local CD signals in achiral material were also found in crescent (C-shaped) gold nanostructures.<sup>2)</sup> These results demonstrate that the established selection rule of optical activity is not valid for local microscopic measurements, and suggest that strongly chiral optical fields are generated in the vicinities of plasmonic materials even if the materials are achiral.

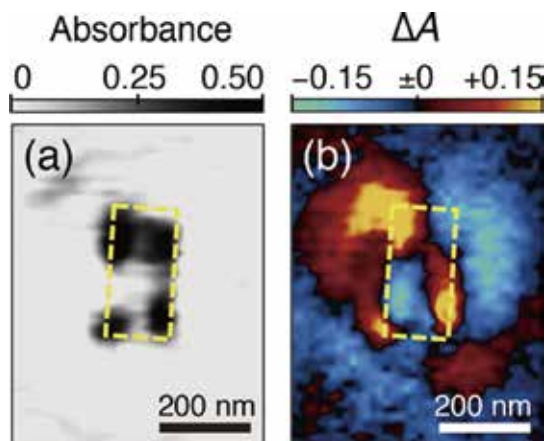


**Figure 2.** Near-field optical images (at 633 nm) of a rectangular gold nanostructure fabricated on a glass substrate via electron beam lithography and lift-off method.<sup>1)</sup> (a) Transmission image. (b) CD image. Dashed yellow lines represent approximate shape of the nanostructure.

### Award

HASHIYADA, Shun; Chemical Society of Japan Student Presentation Award 2015.

## 2. Plasmon Dephasing in Single Gold Nanorods Observed by Ultrafast Near-Field Optical Imaging<sup>3)</sup>

We applied time-resolved near-field optical microscopic measurements with ultrashort light pulses of ~16 fs duration to observe plasmon dephasing processes in single gold nanorods. The correlation width of the time-resolved signal obtained at each position on the nanorod was broadened compared with the auto-correlation width of the pulse, because the plasmon dephasing was convolved on the system response function given by the pulse auto-correlation function. The correlation width maps of the rods (Figure 3) showed spatially oscillating patterns that look similar to the plasmon mode structures observed in the static near-field optical images (as typified with Figure 1). The spatial variation of the correlation widths was explained as arising from the position dependent contribution of the resonant plasmon excitation in the time-resolved signals relative to that of the non-resonant excitation. The dephasing times of the resonant plasmon modes were constant regardless of the excitation position, which is understood to be a consequence of the spatial coherence of the plasmon mode across the rod.

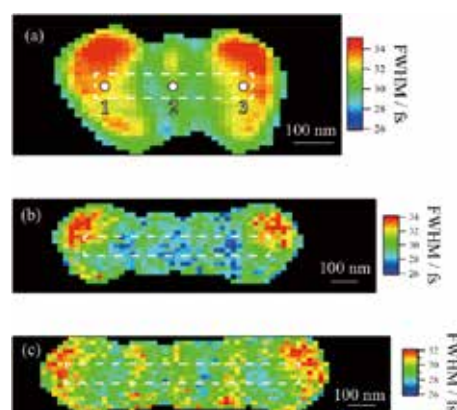


**Figure 3.** Correlation width maps obtained for time-resolved signals of gold nanorods with different dimensions.<sup>3)</sup> Dashed white lines represent approximate shapes of the nanorods. The black parts outside of the nanorods are the areas where the correlation widths were not evaluated because of low signal intensities.

### References

- 1) S. Hashiyada, T. Narushima and H. Okamoto, *J. Phys. Chem. C* **118**, 22229–22233 (2014).
- 2) T. Narushima, S. Hashiyada and H. Okamoto, *ACS Photon.* **1**, 732–738 (2014).
- 3) Y. Nishiyama, K. Imaeda, K. Imura and H. Okamoto, *J. Phys. Chem. C* **119**, 16215–16222 (2015).

\* IMS International Internship Program (Graduate Student from Indian Association for the Cultivation of Science)

† Graduate Student from University of Glasgow

# Exploring Quantum-Classical Boundary

## Department of Photo-Molecular Science Division of Photo-Molecular Science II



**OHMORI, Kenji**  
Professor  
[ohmori@ims.ac.jp]

### Education

1987 B. E. The University of Tokyo  
1992 Ph.D. The University of Tokyo

### Professional Employment

1992 Research Associate, Tohoku University  
2001 Associate Professor, Tohoku University  
2003 Professor, Institute for Molecular Science  
Professor, The Graduate University for Advanced Studies  
2004 Visiting Professor, Tohoku University (–2005)  
2007 Visiting Professor, Tokyo Institute of Technology (–2008)  
2009 Visiting Professor, The University of Tokyo (–2011)  
2012 Visiting Professor, University of Heidelberg  
2014 Visiting Professor, University of Strasbourg

### Awards

1998 Award by Research Foundation for Opto-Science and Technology  
2007 JSPS Prize  
2007 Japan Academy Medal  
2009 Fellow of the American Physical Society  
2012 Humboldt Research Award

### Member

Assistant Professor  
TAKEI, Nobuyuki  
SOMMER, Christian  
IMS Research Assistant Professor  
TANAKA, Akira  
TAKEDA, Shuntaro  
Post-Doctoral Fellow  
GOTO(SHIKANO), Haruka  
Visiting Scientist  
NGUYEN, Quynh\*  
RASTI, Soroush\*  
Graduate Student  
MIZOGUCHI, Michiteru  
KONDO, Norihisa†  
Secretary  
INAGAKI, Itsuko  
YAMAGAMI, Yukiko

**Keywords** Quantum-Classical Boundary, Coherent Control, Attosecond

It is observed in a double-slit experiment by Tonomura and coworkers that single electrons recorded as dots on a detector screen build up to show an interference pattern, which is delocalized over the screen.<sup>1)</sup> This observation indicates that a delocalized wave function of an isolated electron interacts with the screen, which is a bulk solid composed of many nuclei and electrons interacting with each other, and becomes localized in space. This change, referred to as “collapse” in quantum mechanics, is often accepted as a discontinuous event, but a basic question arises: When and how the delocalized wave function becomes localized? Our dream is uncovering this mystery by observing the spatiotemporal evolution of a wave function delocalized over many particles interacting with each other. Having this dream in mind, we have developed coherent control with precisions on the picometer spatial and attosecond temporal scales. Now we apply this ultrafast and ultrahigh-precision coherent control to delocalized wave functions of macroscopic many-particle systems such as an ensemble of ultracold Rydberg atoms and a bulk solid, envisaging the quantum-classical boundary connected smoothly.

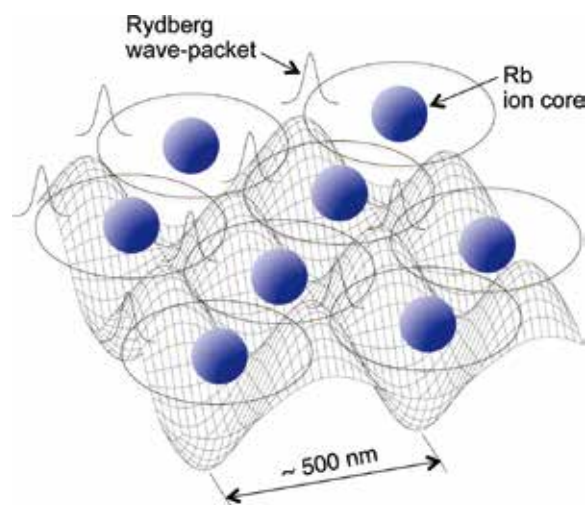


**Figure 1.** Schematic of the many-body system of ultracold Rydberg atoms.<sup>2)</sup>

### Selected Publications

- H. Katsuki *et al.*, “Visualizing Picometric Quantum Ripples of Ultrafast Wave-Packet Interference,” *Science* **311**, 1589–1592 (2006).
- H. Katsuki *et al.*, “Actively Tailored Spatiotemporal Images of Quantum Interference on the Picometer and Femtosecond Scales,” *Phys. Rev. Lett.* **102**, 103602 (2009).
- K. Hosaka *et al.*, “Ultrafast Fourier Transform with a Femtosecond-Laser-Driven Molecule,” *Phys. Rev. Lett.* **104**, 180501 (2010).
- H. Goto *et al.*, “Strong-Laser-Induced Quantum Interference,” *Nat. Phys.* **7**, 383–385 (2011).
- H. Katsuki *et al.*, “All-Optical Control and Visualization of Ultrafast Two-Dimensional Atomic Motions in a Single Crystal of Bismuth,” *Nat. Commun.* **4**, 2801 (2013).
- H. Katsuki *et al.*, “Real-Time Observation of Phase-Controlled Molecular Wave-Packet Interference,” *Phys. Rev. Lett.* **96**, 093002 (2006).

## 1. Manipulation and Visualization of Two-Dimensional Phase Distribution of Vibrational Wave Functions in Solid Parahydrogen Crystal<sup>3)</sup>

Solid parahydrogen, which is known to have an exceptionally long vibrational coherence lifetime as a molecular solid, offers an ideal testbed to perform coherent control experiments in the condensed phase. Here we demonstrate the spatial manipulation and visualization of the relative phase of vibrational wave functions in solid parahydrogen. Spatial distribution of vibrational excitation is generated by femto-second impulsive Raman excitation. It is shown that the imprinted initial phase can be manipulated by wave-front modulation of the excitation laser pulses with a spatial light modulator. An interferometric measurement is used to convert the spatial phase distribution of the vibrational wave functions to the amplitude distribution. We have confirmed that the spatial profile of the scattered anti-Stokes pulse reveals the spatial phase distribution of the wave functions. The read-and-write scheme demonstrated in this experiment is applicable to a broad range of Raman memory systems accessible by  $\Lambda$ -type transitions.

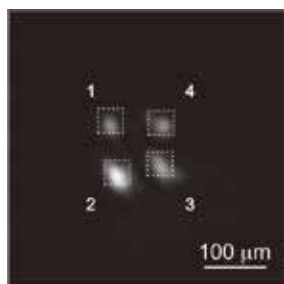


**Figure 2.** (a) O K-edge XAS of liquid water at different positions of liquid layer. Image of the anti-Stokes pulse retrieved by irradiating a probe pulse into the  $p$ -H<sub>2</sub> crystal in which the 2×2 spatial distribution of the wave function is prepared by the impulsive Raman excitation (IRE).

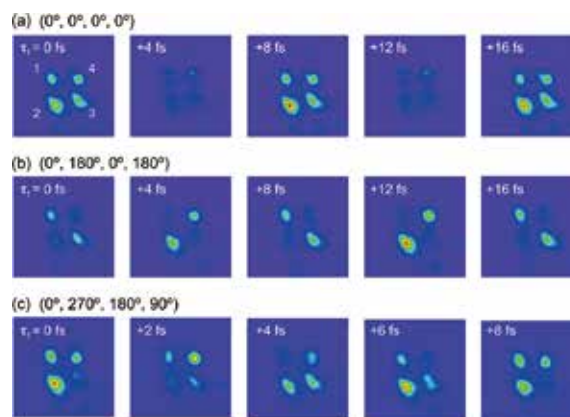


**Figure 3.** False color plots of the temporal evolution of the CCD images of the anti-Stokes pulse as the function of the delay  $\tau_f$  between two IREs. The origin of  $\tau_f$  ( $\tau_f = 0$ ) is arbitrary and is set to 0 for the leftmost panel in each row (a), (b), or (c). The signal is retrieved by the irradiation of a probe pulse at its delay  $\tau_{\text{probe}} \sim 250$  ps. The delay  $\tau_f$  is scanned around 25 ps. The first IRE encodes different relative phases among regions 1–4 shown in Figure 2. Note that the time step for (c) is half of the other two cases.

### References

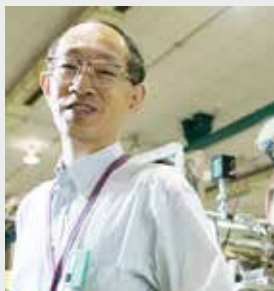
- 1) K. Tonomura *et al.*, *Am. J. Phys.* **57**, 117 (1989).
- 2) K. Ohmori, *Found. Phys.* **44**, 813–818 (2014).
- 3) H. Katsuki *et al.*, *Phys. Rev. B* **92**, 094511 (2015).

\* IMS International Internship Program

† carrying out graduate research on Cooperative Education Program of IMS with Tokyo Institute of Technology

# Local Chemical State Analysis Using Soft X-Rays: Experiment and Theory

Department of Photo-Molecular Science  
Division of Photo-Molecular Science III



**KOSUGI, Nobuhiro**  
Professor  
[kosugi@ims.ac.jp]

#### Education

1976 B.S. Kyoto University  
1981 Ph.D. The University of Tokyo

#### Professional Employment

1981 JSPS Postdoctoral Fellow  
1982 Research Associate, The University of Tokyo  
1988 Lecturer, The University of Tokyo  
1989 Associate Professor, Kyoto University  
1993 Professor, Institute for Molecular Science  
1993 Professor, The Graduate University for Advanced Studies

1996 Visiting Professor, McMaster University, Canada  
2008 Visiting Professor, Université P&M Curie - Paris VI, France  
2011 Visiting Professor, Université Paris-Sud - Paris XI, France  
2013 Visiting Professor, Freie Universität Berlin, Germany

#### Member

Visiting Professor  
AZIZ, Emad F.  
Assistant Professor  
NAGASAKA, Masanari  
YAMANE, Hiroyuki  
JSPS Post-Doctoral Fellow  
YUZAWA, Hayato  
Graduate Student  
TAKEUCHI, Yu\*  
Secretary  
NAKANE, Junko

**Keywords** X-Ray Spectroscopy, Local Chemical State Analysis, Quantum Chemistry

Soft X-rays cannot pass through air or through liquid water due to photoabsorption processes of  $N_2$ ,  $O_2$ , and  $H_2O$  molecules. Such strong interaction of soft X-rays can be used in highly sensitive chemical state analysis of thin samples by X-ray absorption spectroscopy (XAS).

Soft X-rays with photon energies of 100–700 eV excite 1s inner-shell (K-shell) electrons of chemically important light elements such as C, N, and O to unoccupied states of molecules. The 1s electron is localized and bound by an atom in the system but is slightly affected by surrounding atoms and chemical bonds. Therefore, we can select a 1s electron in each atom in molecules by choosing different X-ray energies, and know each atomic component in the unoccupied state in the system. The excited electron in the unoccupied state is also affected by chemical environments. The intermolecular interaction effect is often less than 0.1 eV; therefore, a highly resolved soft X-ray spectrometer is necessary.

In order to realize *in situ* and *in operando* chemical state analysis revealing local electronic structures and weak intermolecular interactions in molecular systems such as organic solids, liquids, aqueous solutions, and molecular clusters, we are developing and improving several kinds of sample cells, detection systems, and spectro-microscopic techniques in X-ray absorption spectroscopy (XAS) for resonant excitation, and resonant and non-resonant X-ray photoelectron spectroscopy (XPS).

We are also using resonant and non-resonant X-ray emission spectroscopy (XES) and angle-resolved photoelectron spectroscopy (ARPES).

Sample thickness should be optimized below 1  $\mu\text{m}$  to get optimal absorbance in XAS. For inhomogeneous samples, the 10 nm-scale spatial resolution is necessary. It is also important to reduce the radiation damage of samples due to strong light-matter interaction in the soft X-ray region.

Highly brilliant soft X-rays for the chemical state analysis are available as synchrotron radiation from in-vacuum undulator-type insertion devices even on low-energy electron storage rings; e.g. 0.75 GeV UVSOR in IMS. In addition to experimental and instrumental developments at UVSOR-III BL3U, BL4U and BL6U, we are developing an original *ab initio* quantum chemical program package GSCF, which is optimized to calculation of molecular inner-shell processes.

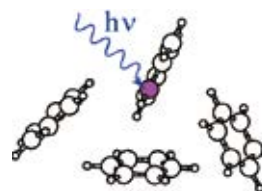


**Figure 1.** The C 1s excitation energy in interacting benzene molecules is dependent and selective on chemically different atomic sites.

#### Selected Publications

- M. Nagasaka, H. Yuzawa, T. Horigome, A. P. Hitchcock and N. Kosugi, "Electrochemical Reaction of Aqueous Iron Sulfate Solutions Studied by Fe L-Edge Soft X-Ray Absorption Spectroscopy," *J. Phys. Chem. C* **117**, 16343–16348 (2013).
- M. Nagasaka, K. Mochizuki, V. Leloup and N. Kosugi, "Local Structures of Methanol-Water Binary Solutions Studied by Soft

X-Ray Absorption Spectroscopy," *J. Phys. Chem. B* **118**, 4388–4396 (2014).

- H. Yamane and N. Kosugi, "Substituent-Induced Intermolecular Interaction in Organic Crystals Revealed by Precise Band Dispersion Measurements," *Phys. Rev. Lett.* **111**, 086602 (5 pages) (2013).

## 1. Optimization of Thin Liquid Layer Samples for Soft X-Ray Absorption Spectroscopy in Transmission Mode

In order to measure soft X-ray absorption spectroscopy (XAS) of liquid samples in transmission mode, it is necessary to optimize thickness of thin liquid layers and reduce non-uniformity of sample thickness in the X-ray absorbed/transmitted region. Recently, we have developed a liquid flow cell, in which the thin liquid layer is sandwiched between two  $\text{Si}_3\text{N}_4$  or  $\text{SiC}$  membranes with Teflon spacers and is pressed by O-rings outside the membranes.<sup>1)</sup> Although the liquid layer is easily assembled by our method, the thickness of liquid layer is not uniform at different positions due to the large window size ( $2 \times 2 \text{ mm}^2$ ). To find the region of the uniform sample thickness in the X-ray absorbed/transmitted region of  $200 \mu\text{m} \times 200 \mu\text{m}$  (determined by our using orifice), we have developed a chamber-type XAS measurement system that is able to scan the sample position, and investigated the influence of the spectral shapes caused by the non-uniform thickness in the O K-edge XAS of liquid water at different sample positions.

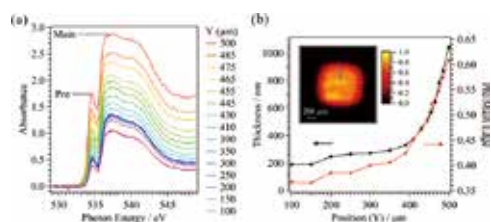


**Figure 2.** (a) O K-edge XAS of liquid water at different sample positions. The pre-edge at 535 eV and the main-edge at 538 eV are shown in the spectra. (b) Thickness of liquid water and Pre/Main ratio of XAS spectra as a function of sample positions. Inset shows the 2D images of the soft X-ray transmission at 550 eV, where the sample positions are scanned as indicated. The size of the present soft X-ray beam is  $200 \mu\text{m} \times 200 \mu\text{m}$ .

Figure 2(a) shows O K-edge XAS spectra of water at different positions of the liquid layer. The liquid thickness at different positions was estimated from the edge-jump of the XAS spectrum. It is also important to determine the intensity ratio of pre-edge at 535 eV to main-edge at 538 eV for the evaluation of the XAS spectra. Figure 2(b) shows the Pre/Main ratio and thickness at different sample positions. The thickness is constant when the sample position is within  $300 \mu\text{m}$  from the center, and is increased when the position exceeds  $300 \mu\text{m}$ . The Pre/Main ratio is nearly constant between 0.36 and 0.40 when the sample thickness is constant, but the Pre/Main ratio is increased at the larger and non-uniform thickness region. This behavior in the Pre/Main ratio is in agreement with the simulated behavior by using the absorbance of water for the non-uniform sample thickness.

### Award

YAMANE, Hiroyuki; The 2014 Young Scientist Award of the Japan Society for Molecular Science.

## 2. Lateral Intermolecular Interaction in Two-Dimensional Superstructure of Organic Monolayers

The intermolecular interaction is a key issue in molecular electronic properties. In the present work, in order to examine the lateral intermolecular interaction in flat-lying molecular layers, we investigated the electronic structure of hexa-*peri*-hexabenzocoronene (HBC) monolayers on Au(111), which forms various superstructures, *e.g.*,  $(5 \times 5)\text{R}0^\circ$ ,  $(3\sqrt{3} \times 3\sqrt{3})\text{R}30^\circ$ , and their mixture, depending on the preparation condition.

Figure 3 shows the low-energy electron diffraction (LEED) image, the surface Brillouin zone (SBZ), and the energy-vs.-momentum  $E(k)$  map of the R0 and R30 phases of the HBC monolayer on Au(111) at 15 K, obtained by angle-resolved photoemission spectroscopy (ARPES). In the R0 phase, the highest occupied molecular orbital (HOMO,  $H_0$ ) disperses in a narrow width by 20 meV only along the  $k_{\Gamma K}$  direction, and the HOMO-1 ( $H_1$ ) disperses by 25 meV only along the  $k_{\Gamma M}$  direction. The opposite trend is observed in the R30 phase; that is, the HOMO disperses by 20 meV along the  $k_{\Gamma M}$  direction, and the HOMO-1 disperses by 25 meV along the  $k_{\Gamma K}$  direction. The observed dispersion and its  $k$  periodicity is dependent not on the substrate SBZ but on the molecular SBZ; therefore, the observed lateral band dispersion rationally arises from a long-range (direct or indirect) intermolecular  $\pi$ - $\pi$  interaction.

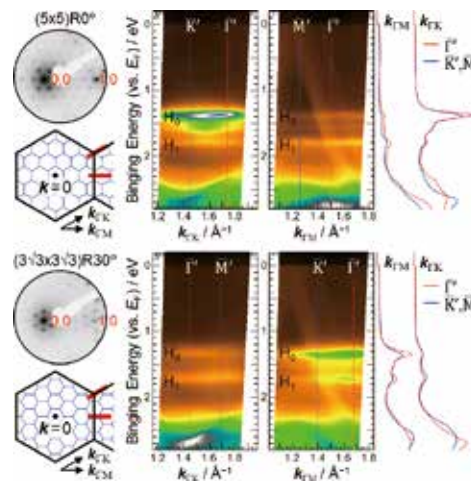


**Figure 3.** LEED, SBZ [black hexagon for Au(111) and blue hexagon for HBC], wherein the red line indicates the scanned region in ARPES, and the  $E(k)$  map of HBC/Au(111) of the R0 and R30 phases at 15 K.

### Reference

- 1) M. Nagasaka *et al.*, *J. Electron Spectrosc. Relat. Phenom.* **177**, 130–134 (2010).

# Electronic Property of Functional Organic Materials

## Department of Photo-Molecular Science Division of Photo-Molecular Science III



**KERA, Satoshi**  
Professor  
[kera@ims.ac.jp]

### Education

1996 B.E. Chiba University  
1998 M.E. Chiba University  
2001 Ph.D. Chiba University

### Professional Employment

1998 JSPS Research Fellow  
2001 Research Associate, Chiba University  
2003 Research Associate, Institute for Molecular Science  
2003 Postdoctoral Fellow, Wuerzburg University  
2004 Assistant Professor, Chiba University  
2007 Associate Professor, Chiba University  
2009 Visiting Associate Professor, Institute for Molecular Science  
2013 Adjunct Lecturer, The Open University of Japan  
2013 Visiting Associate Professor, Soochow University  
2014 Professor, Institute for Molecular Science  
Professor, The Graduate University for Advanced Studies  
Visiting Professor, Chiba University

### Member

Assistant Professor  
UEBA, Takahiro  
Post-Doctoral Fellow  
BUSSOLOTTI, Fabio  
Research Fellow  
KOSWATTAGE, K. Rasika\*  
Graduate Student  
SHIRAIISHI, Ryo  
KIMURA, Kentaro  
YAMAGUCHI, Takuma†  
Secretary  
SHIMIZU, Atsuko

### Keywords

Photoelectron Spectroscopy, Molecular Film, Electronic State

Functional organic materials (FOM) have recently attracted considerable attention both for fundamental research and device applications because of peculiar properties not found in inorganics and small molecules. However the mechanisms and its origin of various device characteristics are still under debate. Scientific mysteries would be raised because people have believed that electronic structure of FOM would be conserved as in an isolated molecule for solid phases due to van der Waals interaction. To reveal characteristics of FOM the key investigation would be on precise experiments on the electronic structure at various interfaces, including organic–organic and organic–inorganic (metal/semiconductor) contacts. In these systems, the impacts of weak interaction on the electronic structure would be appeared as small intensity modulation of photoelectron-emission fine features depending on adsorption and aggregation on the surface. By recent development in the instrumental we can assess hidden fine structures in the electronic states, *e.g.* electron–phonon coupling, quasi-particle states, very small gap-state DOS, weak band dispersion and dynamic electronic polarization. To elucidate what really happens for the FOM at the interface upon weak interaction, an evaluation on the wave-function

spread of the electronic states would be very important because the interface states for the physisorbed systems are described to be a delocalized molecular orbital state depending on the strength of weak electronic coupling (hybridization). Seeing a modification of electron wave function upon weak electronic coupling as well as strong electron–phonon coupling is central issue on our agenda.

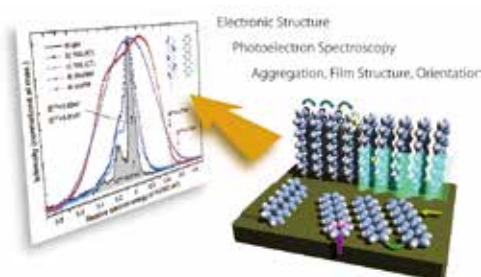


**Figure 1.** Scheme of a rich assortment in the structure of functional molecular materials and variety in the spectral feature of ultraviolet photoelectron spectrum (UPS) for the HOMO band taken for various structural phases (gas-phase, lying monolayers, standing monolayer, and disordered film).

### Selected Publications

- F. Busolotti, S. Kera, K. Kudo, A. Kahn and N. Ueno, “Gap States in Pentacene Thin Film Induced by Inert Gas Exposure,” *Phys. Rev. Lett.* **110**, 267602 (5 pages) (2013).
- S. Duhm, Q. Xin, S. Hosoumi, H. Fukagawa, K. Sato, N. Ueno and S. Kera, “Charge Reorganization Energy and Small Polaron Binding Energy of Rubrene Thin Films by Ultraviolet Photoelectron

Spectroscopy,” *Adv. Mater.* **24**, 901–905 (2012).

- S. Kera, H. Yamane and N. Ueno, “First Principles Measurements of Charge Mobility in Organic Semiconductors: Valence Hole-Vibration Coupling in Organic Ultrathin Films,” *Prog. Surf. Sci.* **84**, 135–154 (2009).

## 1. Charge Reorganization Energy and Small Polaron Energy of Molecular Films<sup>1)</sup>

Understanding of electron–phonon coupling as well as intermolecular interaction is required to discuss the mobility of charge carrier in functional molecular solids. We summarized recent progress in direct measurements of valence hole-vibration coupling in ultrathin films of organic semiconductors by using ultraviolet photoelectron spectroscopy (UPS). The experimental study of hole-vibration coupling of the highest occupied molecular orbital (HOMO) state in ordered monolayer film by UPS is essential to comprehend hole-hopping transport and small-polaron related transport in organic semiconductors. Only careful measurements can attain the high-resolution spectra and provide key parameters in hole-transport dynamics, namely the charge reorganization energy and small polaron binding energy. Analyses methods of the UPS-HOMO fine feature and resulting charge reorganization energy and small polaron binding energy are described for pentacene and perfluoropentacene films. Difference between thin-film and gas-phase results is discussed by using newly measured high-quality gas-phase spectra of pentacene. Methodology for achieving high-resolution UPS measurements for molecular films is also described.

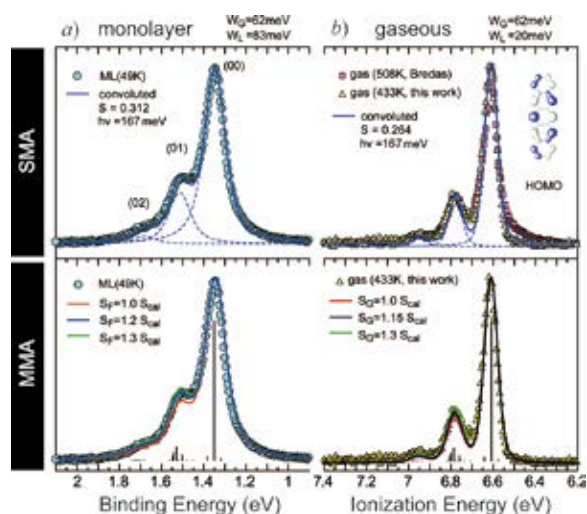


**Figure 2.** Comparison of HOMO band of pentacene between angle-integrated UPS for the monolayer (*a*, left panels) and gas-phase UPS (*b*, right panels). Convoluted curves by the single mode (SMA) and multimode (MMA) analyses of vibration coupling are also shown.

## 2. Impact of Molecular Orbital Distribution on Photoelectron Intensity<sup>2)</sup>

Ultraviolet photoelectron spectroscopy (UPS) is well

established technique for studying the electronic structure of surfaces and interfaces. In the detail, however, the origins of the UPS spectral features are not clearly understood even for so-called van-der Waals molecular crystals formed by weak intermolecular interaction. For molecular monolayer films prepared on a metal substrate, the spectrum is complicated much more due to orbital hybridization and charge transfer, which lead to interface states and/or broadening of spectral features. In principle, photoelectrons can give us all of important information on electronic properties in the molecular systems, when we measure precisely the molecular sample prepared very carefully.

The recent development in the theoretical evaluation of photoelectron intensity from  $\pi$ -electronic states delocalized over a molecule is discussed. By comparing the experimental photoelectron angular distribution (PAD) from the organic molecular assemblies with computed PAD we show that the use of the initial-state orbitals by density functional theory and the final continuum states by multiple-scattering theory (MSMO) is suited for simulations of angle-resolved UPS (ARUPS) and PAD. We demonstrate that the ARPES and PAD simulations are useful to characterize the top five  $\pi$ -electronic states for picene ( $C_{22}H_{14}$ ) film.

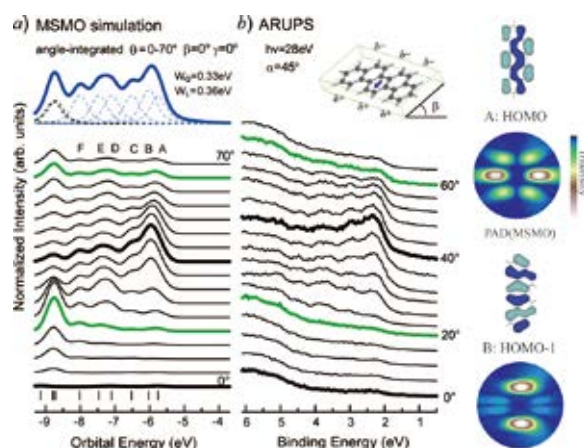


**Figure 3.** (a) Simulated ARUPS by MSMO calculation for an isolated picene molecule. (b) Observed take-off angle  $\theta$  dependence of ARUPS of picene film (10 nm) on graphite. The molecules are assumed to be lying-flat in the film. Each spectrum is produced by convoluting Voigt function for all states. Calculated PADs of top two MO states by MSMO are shown (right).

## References

- 1) S. Kera and N. Ueno, *J. Electron Spectrosc. Relat. Phenom.* **204**, 2–11 (2015).
- 2) Y. Liu, D. Ikeda, S. Nagamatsu, T. Nishi, N. Ueno and S. Kera, *J. Electron Spectrosc. Relat. Phenom.* **195**, 287–292 (2014).

\* from Chiba University

† carrying out graduate research on Cooperative Education Program of IMS with Chiba University

# Light Source Developments by Using Relativistic Electron Beams

## UVSOR Facility Division of Advanced Accelerator Research



**KATOH, Masahiro**  
Professor  
[mkatoh@ims.ac.jp]

### Education

1982 B.S. Tohoku University  
1997 Ph.D. Tohoku University

### Professional Employment

1986 Research Associate, National Laboratory for High Energy Physics  
2000 Assistant Professor, Institute for Molecular Science  
2004 Professor, Institute for Molecular Science  
Professor, The Graduate University for Advanced Studies

### Member

Assistant Professor  
KONOMI, Taro\*  
IMS Fellow  
MIRIAN, Najmeh Sadat  
Graduate Student  
ITO, Kenya†  
OODAKE, Daichi†

**Keywords** Accelerator, Synchrotron Radiation, Free Electron Laser

UVSOR is a synchrotron light source to provide low energy synchrotron light ranging from terahertz wave to soft X-rays. Although it was constructed about 30 years ago, its performance is still in the world top level. This is the result of the continuous effort on improving the machine. Our research group has been developing accelerator technologies toward producing bright and stable synchrotron light, such as high brightness electron beam optics, novel insertion devices or state-of-the-art beam injection technique. We have been also developing novel light source technologies toward producing synchrotron radiation with various characteristics such as free electron laser, coherent synchrotron radiation and laser Compton gamma-rays. We are also investigating future light sources for the facility, such as a diffraction limited light source or a linac-based free electron laser source.



**Figure 1.** UVSOR-III Electron Storage Ring and Synchrotron Radiation Beamlines.

### Selected Publications

- S. Bielawski, C. Evain, T. Hara, M. Hosaka, M. Katoh, S. Kimura, A. Mochihashi, M. Shimada, C. Szwaj, T. Takahashi and Y. Takashima, "Tunable Narrowband Terahertz Emission from Mastered Laser-Electron Beam Interaction," *Nat. Phys.* **4**, 390–393 (2008).
- M. Shimada, M. Katoh, M. Adachi, T. Tanikawa, S. Kimura, M. Hosaka, N. Yamamoto, Y. Takashima and T. Takahashi, "Transverse-Longitudinal Coupling Effect in Laser Bunch Slicing," *Phys. Rev. Lett.* **103**, 144802 (2009).
- T. Tanikawa, M. Adachi, H. Zen, M. Hosaka, N. Yamamoto, Y. Taira and M. Katoh, "Observation of Saturation Effect on Vacuum Ultraviolet Coherent Harmonic Generation at UVSOR-II," *Appl. Phys. Express* **3**, 122702 (3 pages) (2010).
- Y. Taira, M. Adachi, H. Zen, T. Tanikawa, N. Yamamoto, M. Hosaka, Y. Takashima, K. Soda and M. Katoh, "Generation of Energy-Tunable and Ultrashort-Pulse Gamma Ray via Inverse Compton Scattering in an Electron Storage Ring," *Nucl. Instrum. Methods Phys. Res., Sect. A* **652**, 696–700 (2011).
- I. Katayama, H. Shimosato, M. Bito, K. Furusawa, M. Adachi, M. Shimada, H. Zen, S. Kimura, N. Yamamoto, M. Hosaka, M. Katoh and M. Ashida, "Electric Field Detection of Coherent Synchrotron Radiation in a Storage Ring Generated Using Laser Bunch Slicing," *Appl. Phys. Lett.* **100**, 111112 (2012).
- Y. Taira, H. Toyokawa, R. Kuroda, N. Yamamoto, M. Adachi, S. Tanaka and M. Katoh, "Photon-Induced Positron Annihilation Lifetime Spectroscopy Using Ultrashort Laser-Compton-Scattered Gamma-Ray Pulses," *Rev. Sci. Instrum.* **84**, 053305 (2013).

## 1. Light Source Technology Developments Based on Laser and Synchrotron

We have developed novel light source technologies using UVSOR-III electron storage ring and external laser sources. Under the support of Quantum Beam Technology Program of JST/MEXT, a new experimental station dedicated for the source development studies were constructed. We modified a part of the accelerator to produce a space for new undulator system and dedicated beam-lines. The generation of coherent synchrotron radiation based on our original method was successfully demonstrated at the new site, in collaboration with Lille Univ. and Nagoya Univ. For the applications using coherent synchrotron radiation, the construction of the beam-line is in progress. Some basic researches on the optical vortex beam from helical undulators are in progress in collaboration with Hiroshima Univ. and KEK.

Laser Compton scattering is a method to produce monochromatic and energy-tunable gamma-ray pulses. Laser pulses are injected to the storage ring and are scattered by the relativistic electrons circulating in the ring. We developed a unique method to produce ultra-short gamma-ray pulses in pico- and femtosecond range for the first time and demonstrated its potential as a powerful tool for material sciences by a photon-induced positron annihilation lifetime spectroscopy experiment, in collaboration with AIST. We have started developing an imaging technology for isotopes based on nuclear fluorescence resonance in collaboration with Kyoto Univ., AIST and JAEA. We have succeeded in producing intense gamma-ray beam by using a fiber laser. We have started reconstructing the resonator free electron laser on UVSOR-III, which will be used to produce intense gamma-rays through intra-cavity inverse Compton scattering.



**Figure 2.** Twin Polarization-variable Undulators/Optical Klystron at UVSOR-III.

## 2. Accelerator Technology Developments for Synchrotron Light Source and Free Electron Laser

The UVSOR facility has been operational as a national synchrotron light source for lower energy photons from the terahertz wave to the soft X-rays. The machine was born as a low energy second generation light source and now it is 30 years old. We have proposed several upgrades and most of them have been carried out successfully. We designed a special electron beam optics intended to higher brightness. We designed accelerator components necessary for the new optics and have successfully remodeled and commissioned the machine with the new optics. We have designed six undulators and have successfully installed and commissioned all of them. We have succeeded in introducing a novel operation mode called Top-up operation, in which the electron beam intensity is kept quasi-constant at a high beam current, 300 mA. As the result of all these efforts, now, the machine is the brightest synchrotron light sources among the low energy machines below 1 GeV in the world.

We continue the efforts to improve the machine performance by using new technologies such as pulsed sextupole injection scheme. Also, we are designing new accelerators for future project of the facility, such as linear accelerator based free electron laser or diffraction limited storage ring light source. As a technology development towards the new facility, a superconducting RF electron gun has been developed in collaboration with KEK, which would produce high brightness electron beam with high repetition rate.



**Figure 3.** Optical Cavity for Resonator Free Electron Laser is under reconstruction at UVSOR-III.

### Award

ITO, Kenya; 2015 Annual Meeting Award of the Particle Accelerator Society of Japan.

\* Present Address; High Energy Accelerator Research Organization

† carrying out graduate research on Cooperative Education Program of IMS with Nagoya University

# Angle-Resolved Photoemission Study on Strongly Correlated Electron Materials

UVSOR Facility  
Division of Advanced Solid State Physics



**TANAKA, Kiyohisa**  
Associate Professor  
[k-tanaka@ims.ac.jp]

#### Education

1990 B.S. The University of Tokyo  
2005 Ph.D. The University of Tokyo

#### Professional Employment

2005 Postdoctoral Fellow, Stanford University and Lawrence Berkeley National Laboratory  
2008 Assistant Professor, Osaka University  
2013 Associate Professor, Osaka University  
2014 Associate Professor, Institute for Molecular Science  
Associate Professor, The Graduate University for Advanced Studies

#### Member

Assistant Professor  
MATSUNAMI, Masaharu\*  
IDETA, Shin-Ichiro  
Graduate Student  
KOUCHI, Shogo†  
SUGIHARA, Shintarou†  
OHNO, Yuuki‡  
SOBIREY, Tilman Lennart‡

**Keywords** Strongly Correlated Electron System, Synchrotron Light, Photoemission

Strongly correlated electron materials has attracted more attentions in the last few decades because of their unusual and fascinating properties such as high- $T_c$  superconductivity, giant magnetoresistance, heavy fermion and so on. Those unique properties can offer a route toward the next-generation devices. We investigate the mechanism of the physical properties as well as the electronic structure of those materials by using angle-resolved photoemission spectroscopy (ARPES), a powerful tool in studying the electronic structure of complex materials, based on synchrotron radiation.

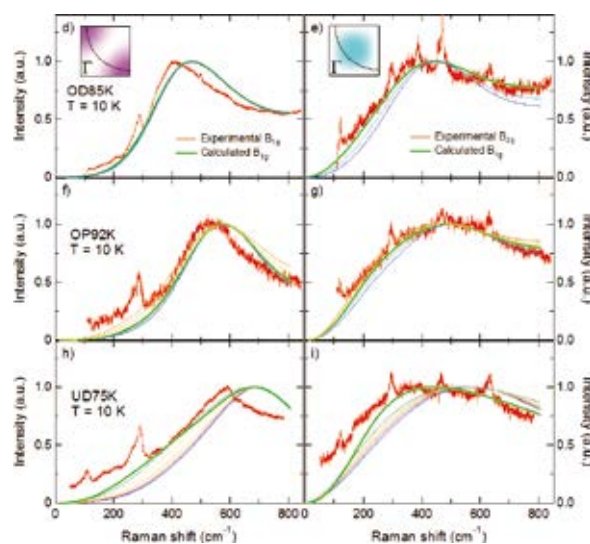


**Figure 1.** Calculation results of Bi2212 for  $B_{1g}$  and  $B_{2g}$  ERS spectra using ARPES spectra together with experimental ones.

#### Selected Publications

- K. Tanaka, T. Yoshida, A. Fujimori, D. H. Lu, Z.-X. Shen, X.-J. Zhou, H. Eisaki, Z. Hussain, S. Uchida, Y. Aiura, K. Ono, T. Sugaya, T. Mizuno and I. Terasaki, "Effects of Next-Nearest-Neighbor Hopping  $t'$  on the Electronic Structure of Cuprates," *Phys. Rev. B* **70**, 092503 (4 pages) (2004).
- K. Tanaka, W. S. Lee, D. H. Lu, A. Fujimori, T. Fujii, Risdiana, I. Terasaki, D. J. Scalapino, T. P. Devereaux, Z. Hussain and Z.-X. Shen, "Distinct Fermi-Momentum-Dependent Energy Gaps in Deeply Underdoped Bi2212," *Science* **314**, 1910–1913 (2006).
- W. S. Lee, I. M. Vishik, K. Tanaka, D. H. Lu, T. Sasagawa, N. Nagaosa, T. P. Devereaux, Z. Hussain and Z.-X. Shen, "Abrupt Onset of a Second Energy Gap at the Superconducting Transition of Underdoped Bi2212," *Nature* **450**, 81–84 (2007).
- E. Uykur, K. Tanaka, T. Masui, S. Miyasaka and S. Tajima, "Coexistence of the Pseudogap and the Superconducting Gap Revealed by the  $c$ -Axis Optical Study of  $YBa_2(Cu_{1-x}Zn_x)O_{7-\delta}$ ," *J. Phys. Soc. Jpn.* **82**, 033701 (4 pages) (2013).

## 1. Quantitative Comparison between ARPES and ERS on High- $T_c$ Cuprate Superconductor

Both of ARPES and electronic Raman scattering (ERS) revealed two energy scales for the gap in different momentum spaces in the cuprates. However, the interpretations were different and the gap values were also different in two experiments. In order to clarify the origin of these discrepancies, we have directly compared experimental ARPES and ERS by using new calculation method of ERS through the Kubo formula.

It is well known that ARPES intensity is a function of matrix element, Fermi Dirac function and a spectral function  $A(k, \omega)$ . On the other hand, the electronic Raman response in the superconducting state can be described by Green's functions using the Kubo susceptibility. Since the imaginary part of Green's function is the spectral function, the electronic Raman responses can be calculated from ARPES spectra.

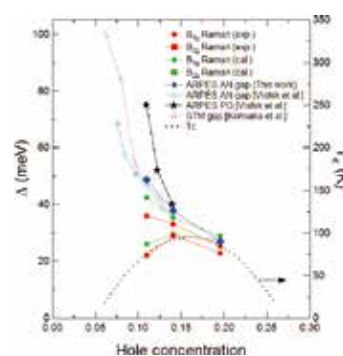
In this study, we have prepared  $\text{Bi}_2\text{Sr}_2\text{CaCu}_2\text{O}_{8+\delta}$  (Bi2212) samples with three doping levels, namely, underdoped (UD75K:  $T_c = 75$  K), optimally doped (OP92K:  $T_c = 92$  K), and overdoped (OD85K:  $T_c = 85$  K) samples and performed ARPES and ERS measurements on the same sample to directly compare the results. From ARPES spectra, we obtained  $A(k, \omega)$  and calculated ERS spectra and compared to the experimental ERS spectra.

Figure 1 shows the calculated ERS spectra with different intensity distribution of  $A(k, \omega)$  along the Fermi surface. Compared to the conventional ERS spectral calculation based on kinetic theory, our new calculation results reproduced spectral features much better (not shown). Especially  $B_{2g}$  spectra, which are sensitive to the nodal region in the momentum space, were well reproduced. Doping dependence of the best fitted intensity distribution of  $A(k, \omega)$  shows that the spectral function confined in the nodal region distributes to the antinodal region as the doping level increases.

The peak energies of the calculated Raman spectra were plotted in Figure 2 together with the experimental Raman, ARPES and STM data. From  $B_{1g}$  spectra, which are sensitive to the antinodal region in the momentum space, we found that the ARPES antinodal gap is always larger than the experimental  $B_{1g}$  peak energy. Since the difference increases with underdoping, this difference is possibly caused by the pseudogap. In Figure 2, we also plotted the pseudogap energy determined by ARPES Bi2212 data taken at 100 K. The pseudogap increases rapidly with underdoping and it seems that the superconducting gap in ARPES is enhanced by underlying-high-energy-pseudogap.

The present results give us the following important messages. First, Raman and ARPES can be understood with the same gap profile. Namely, the nodal slope of gap profiles is doping independent, as reported by ARPES. The apparent doping dependence of the  $B_{2g}$  peak energy is caused by the change of spectral weight of  $A(k, \omega)$  along the Fermi surface.

Second, the antinodal gap of ARPES is a superconducting gap that is strongly affected by the pseudogap, whereas the Raman  $B_{1g}$  gap is moderately affected. This probe-dependent effect of the pseudogap is the main source for the difference between the Raman  $B_{1g}$  gap and the ARPES antinodal gap energies. Third, while the spectral weight of  $A(k, \omega)$  is confined into the nodal region in the underdoped sample, the antinodal region gains spectral weight with doping and contributes to superconductivity. Although this is similar to the "Fermi arc" picture reported before, the Fermi surface area contributing to superconductivity in our results is larger than the Fermi arc area estimated from the normal state. All these findings reflect the unusual electronic states where superconductivity and pseudogap coexist even at the lowest temperature.



**Figure 2.** Doping dependence of the peak energies in Bi2212 obtained from ERS calculations in comparison to the experimental data from Raman, ARPES and STM measurements.

## 2. Development of New Spin-Resolved ARPES

UVSOR Facility in Institute for Molecular Science equips two public undulator-beamlines for ARPES: BL5U in the photon energy  $h\nu$  region of 20–200 eV and BL7U of  $h\nu = 6$ –40 eV. Since the monochromator of BL5U is an old-style spherical grating type SGM-TRAIN constructed in 1990s and the throughput intensity and energy resolution are poor, the beamline was planned to be replaced to state-of-the-art monochromator and end station with spin-resolved ARPES. The newly developed electron lens system successfully achieved  $\sim 100$  times better momentum resolution perpendicular to slit direction compared to the conventional ARPES. The beamline will be open to users from FY2016.

### References

- 1) K. Tanaka, W. S. Lee, D. H. Lu, A. Fujimori, T. Fujii, Risdiana, I. Terasaki, D. J. Scalapino, T. P. Devereaux, Z. Hussain and Z.-X. Shen, *Science* **314**, 1910–1913 (2006).
- 2) N. T. Hieu, K. Tanaka, T. Masui, S. Miyasaka, S. Tajima and T. Sasagawa, *Phys. Procedia* **45**, 41–44 (2013).

\* Present Address; Toyota Technological Institute

† carrying out graduate research on Cooperative Education Program of IMS with Nagoya University

‡ carrying out graduate research on Cooperative Education Program of IMS with Osaka University

# Electronic Structure and Decay Dynamics Following Core Hole Creation in Molecules

UVSOR Facility  
Division of Advanced Photochemistry



**SHIGEMASA, Eiji**  
Associate Professor  
[sigemasa@ims.ac.jp]

#### Education

1986 B.S. Hiroshima University  
1988 M.S. Osaka University  
1997 Ph.D. The University of Tokyo

#### Professional Employment

1990 Research Associate, National Laboratory for High Energy Physics  
1997 CEA Researcher, LURE, Université de Paris-Sud  
1999 Associate Professor, Institute for Molecular Science  
2007 Associate Professor, The Graduate University for Advanced Studies

#### Member

Assistant Professor  
IWAYAMA, Hiroshi

**Keywords** Soft X-Ray Spectroscopy, Inner-Shell Excitation, Photodissociation Dynamics

The detailed comprehension of the electronic structure of molecules is an important step toward understanding the chemical and physical properties of matter, and also provides a link between atomic and solid-state physics. Information on photoexcitation, photoionization, and photodissociation processes derived from molecular spectroscopy is of fundamental importance, and also useful in various scientific disciplines, including astrophysics, planetary sciences, radiation chemistry, and biology.

Synchrotron radiation combined with a suitable monochromator is a powerful research tool for systematic investigations of outer- and inner-shell excitation and ionization processes in molecules, because the spectral range matches the binding energies of the valence and core electrons of the elements which form molecules of physical and chemical interest, namely low-Z molecules. In order to promote inner-shell electrons of low-Z molecules efficiently, it is indispensable to utilize monochromatized synchrotron radiation in the soft X-ray region.

Inner-shell excited states of low-Z molecules relax mainly through Auger decay, leading to the formation of highly excited singly or multiply charged molecular ions with outer-shell holes. These molecular ions are in general quite unstable, and immediately break apart into fragment ions and neutrals.

The electronic relaxation and dissociation processes are coupled, and depend on the electronic and geometrical structure of the molecules.

The major aim for investigating molecular inner-shell excitation is to determine what happens to molecules following the excitation and ionization of an inner-shell electron by using various spectroscopic techniques to define the initial photoexcitation process itself, and to characterize and correlate the electrons, ions, neutrals, and metastables that are produced as a result.

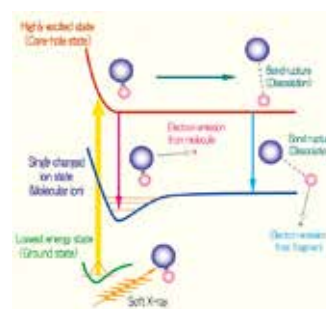


**Figure 1.** Schematic representation of the potential energy curves associated with the inner-shell excitation and subsequent de-excitation processes.

#### Selected Publications

- E. Shigemasa and N. Kosugi, "Molecular Inner-Shell Spectroscopy. ARPIS Technique and its Applications," in *Advances in Chemical Physics*, Eds., S.A. Rice and A. Dinner, Wiley; New York, **Vol. 147**, p. 75–126 (2011).
- M. N. Piancastelli, R. Guillemin, M. Simon, H. Iwayama and E. Shigemasa, "Ultrafast Dynamics in C 1s Core-Excited CF<sub>4</sub> Revealed by Two-Dimensional Resonant Auger Spectroscopy," *J. Chem. Phys.* **138**, 234305 (5 pages) (2013).

## 1. Ultrafast Dissociation of Inner-Shell Excited CF<sub>4</sub> Molecules Studied by an Auger-Electron–Ion Coincidence Method

Recently, we found a signature of ultrafast dissociation following C 1s  $\rightarrow \sigma^*(t_2)$  core excitation in CF<sub>4</sub> by using two dimensional electron spectroscopy.<sup>1)</sup> We observed Auger electrons from both CF<sub>3</sub><sup>\*</sup> fragment and CF<sub>4</sub><sup>\*</sup> parent molecule. This means that the Auger decay and dissociation processes take place on the same time scale and significantly compete with each other. In the current study, we have investigated anisotropic angular distributions of ejected CF<sub>3</sub><sup>+</sup> ions by using an Auger-electron–ion coincidence method. Since the CF bond involved in the C 1s  $\rightarrow \sigma^*(t_2)$  core excitation is immediately broken due to the ultrafast dissociation, anisotropic angular distributions of ejected the CF<sub>3</sub><sup>+</sup> ions are expected.

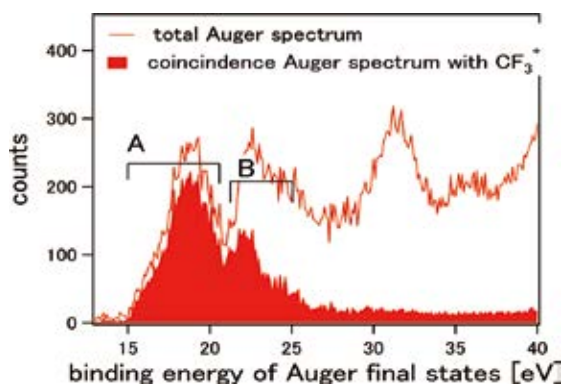


**Figure 2.** Non-coincident and coincident Auger electron spectra with CF<sub>3</sub><sup>+</sup> ions.

The Auger-electron–ion coincidence measurements were carried out on the undulator beamline BL6U at UVSOR. The radiation from an undulator was monochromatized by a variable included angle varied line-spacing plane grating monochromator. The electrons ejected at 54.7° with respect to the electric vector of the incident radiation were analyzed in energy by a double toroidal analyzer (DTA), while ions were extracted from the interaction region into a momentum spectrometer by a pulsed electric field according to the electron detection. Arrival position on the detector and time-of-flights of ions were recorded for every event. The pass energy of the DTA was set to 200 eV for observing the Auger electrons. The energy resolution was about 1.9 eV.

Figure 2 shows non-coincident and coincidence Auger spectra with CF<sub>3</sub><sup>+</sup> ions. It is seen that the CF<sub>3</sub><sup>+</sup> ions are coincident with electrons at the binding energy of 15 ~ 25 eV, where two peaks A and B are detected. For higher binding energies, we observed smaller fragment ions such as CF<sub>2</sub><sup>+</sup>, CF<sup>+</sup> and C<sup>+</sup> (not shown here). From the previous work,<sup>1)</sup> the peaks A and B are attributable to the Auger electrons from the CF<sub>3</sub><sup>\*</sup> fragment and CF<sub>4</sub><sup>\*</sup> parent molecules, respectively.

Figures 3(a) and 3(b) show ion images of CF<sub>3</sub><sup>+</sup> fragments, which were taken in coincident with electrons at the peaks A and B, respectively. The angular distribution of CF<sub>3</sub><sup>+</sup> ions is considerably anisotropic in Figure 3(a), while almost isotropic

angular distributions are seen in Figure 3(b). Two island-like structures along the polarization vector are clearly observed in Figure 3(a). This means that the core-excited CF<sub>4</sub> molecules lead to immediate CF bond breaking, which is the direct evidence of the ultrafast dissociation for the peak A. The detailed data analyses are now in progress.

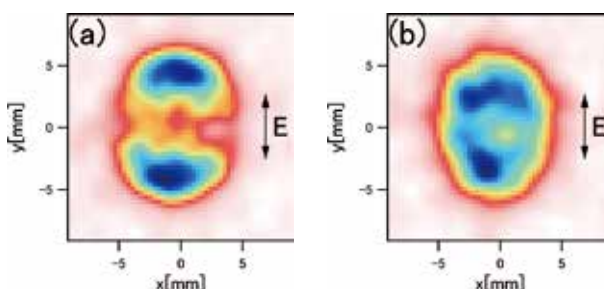


**Figure 3.** Ion images of CF<sub>3</sub><sup>+</sup> ions taken in coincident with Auger electrons at (a) peak A and (b) peak B.

## 2. Photoionization of Helium Atoms by Higher Harmonic Radiation from a Helical Undulator

The  $n_{\text{th}}$  harmonic radiation from a helical undulator carries orbital angular momentum (OAM) of  $(n-1)\hbar$  per photon.<sup>2,3)</sup> This accelerator-based method efficiently generates the OAM photon beam in a wide wavelength range. As a first step of the application study of the OAM photon beam, we have investigated the interaction of the OAM photon and gas-phase atoms in which violation of the dipole selection rules is predicted.<sup>4)</sup>

The experiments were performed at the undulator beamline BL1U during the machine study operations. We observed the angular distributions of the He 1s photoelectrons by using an imaging spectrometer. The downstream part of the tandem APPLE-II undulators was used with horizontal and circular polarization modes. The OAM photon beams were obtained as the 2nd and 3rd harmonic radiation in the circular polarization mode.

Concerning the horizontal polarization and the fundamental radiation with circular polarization, the photoelectron angular distributions measured are fairly in agreement with those calculated by assuming the normal dipole transition. This confirms the validity of the analyzing procedure in the present study. The analysis of the photoionization by the OAM photon is in progress. Although preliminary result indicates the slight deviation from the dipole selection rule in the OAM photoionization, it is required to perform more precise measurements for unveiling the influence of the OAM photon.

### References

- 1) M. N. Piancastelli, R. Guillemin, M. Simon, H. Iwayama and E. Shigemasa, *J. Chem. Phys.* **138**, 234305 (5 pages) (2013).
- 2) S. Sasaki and I. McNulty, *Phys. Rev. Lett.* **100**, 124801 (2008).
- 3) J. Bahrtdt *et al.*, *Phys. Rev. Lett.* **111**, 034801 (2013).
- 4) A. Picón *et al.*, *New J. Phys.* **12**, 083053 (2010).

# Micro Solid-State Photonics

## Laser Research Center for Molecular Science Division of Advanced Laser Development



**TAIRA, Takunori**  
Associate Professor  
[taira@ims.ac.jp]

### Education

1983 B.A. Fukui University  
1985 M.S. Fukui University  
1996 Ph.D. Tohoku University

### Professional Employment

1985 Researcher, Mitsubishi Electric Corp.  
1989 Research Associate, Fukui University  
1993 Visiting Researcher, Stanford University (–1994)  
1998 Associate Professor, Institute for Molecular Science  
Associate Professor, The Graduate University for Advanced Studies

### Awards

2004 Persons of Scientific and Technological Research Merits, Commendation by Minister of Education, Culture, Sports, Science and Technology, Japan  
2010 OSA Fellow Award, The Optical Society (OSA)  
2012 SPIE Fellow Award, The International Society for Optical Engineering (SPIE)  
2014 IEEE Fellow Award, The Institute of Electrical and Electronics Engineers (IEEE)

### Member

Assistant Professor  
ISHIZUKI, Hideki  
IMS Fellow  
ARZAKANTSYAN, Mikayel  
Post-Doctoral Fellow  
TSUNEKANE, Masaki  
SATO, Yoichi  
ZHENG, Lihe  
YAHIA, Vincent  
LIM, Hwanhong  
Research Fellow  
KAUSAS, Arvydas  
Secretary  
ONO, Yoko  
INAGAKI, Yayoi

### Keywords

Solid-State Lasers, Nonlinear Optics, Micro Solid-State Photonics

“Micro Solid-State Photonics,” based on the micro domain structure and boundary controlled materials, opens new horizon in the laser science. The engineered materials of micro and/or microchip solid-state, ceramic and single-crystal, lasers can provide excellent spatial mode quality and narrow linewidths with enough power. High-brightness nature of these lasers has allowed efficient wavelength extension by nonlinear frequency conversion, UV to THz wave generation. Moreover, the quasi phase matching (QPM) is an attractive technique for compensating phase velocity dispersion in frequency conversion. The future may herald new photonics.

Giant pulse > 10 MW was obtained in 1064nm microchip lasers using micro-domain controlled materials. The world first laser ignited gasoline engine vehicle, giant-pulse UV (355 nm, 266 nm) and efficient VUV (118 nm) pulse generations have been successfully demonstrated. Also, few cycle mid-IR pulses for atto-second pulses are demonstrated by LA-PPMgLN. We have developed new theoretical models for the micro-domain control of anisotropic laser ceramics. These functional micro-domain based highly brightness/brightness-temperature compact lasers and nonlinear optics, so to speak “Giant Micro-



**Figure 1.** Giant micro-photonics.

photonics,” are promising. Moreover, the new generation of micro and/or microchip lasers by using orientation-controlled advanced ceramics can provide extreme high performances in photonics.

### Selected Publications

- H. Sakai, H. Kan and T. Taira, “>1 MW Peak Power Single-Mode High-Brightness Passively Q-Switched Nd<sup>3+</sup>:YAG Microchip Laser,” *Opt. Express* **16**, 19891–19899 (2008).
- M. Tsunekane, T. Inohara, A. Ando, N. Kido, K. Kanehara and T. Taira, “High Peak Power, Passively Q-Switched Microlaser for Ignition of Engines,” *IEEE J. Quantum Electron.* **46**, 277–284 (2010).
- T. Taira, “Domain-Controlled Laser Ceramics toward Giant Micro-

Photonics,” *Opt. Mater. Express* **1**, 1040–1050 (2011).

- H. Ishizuki and T. Taira, “Half-Joule Output Optical-Parametric Oscillation by Using 10-mm-Thick Periodically Poled Mg-Doped Congruent LiNbO<sub>3</sub>,” *Opt. Express*, **20**, 20002–20010 (2012).
- R. Bhandari, N. Tsuji, T. Suzuki, M. Nishifuji and T. Taira, “Efficient Second to Ninth Harmonic Generation Using Megawatt Peak Power Microchip Laser,” *Opt. Express* **21**, 28849–28855 (2013).

## 1. Anisotropic Yb:FAP Laser Ceramics by Micro-Domain Control

Highly transparent Yb:FAP fluorapatite (FAP) ceramics were realized by use of slip casting under rotational magnetic field of 1.4 T from a electromagnet, even though the main crystal axis become a hard magnetization axis. This means that the enhancement of magnetic anisotropy by rare-earth doping is also effective for the orientation control even under the rotating magnetic field. X-ray and optical evaluations clearly gives the first evidence that our Yb:FAP ceramics have a laser-grade quality in the world. We confirmed the laser-grade quality of Yb:FAP ceramics by inserting into a lasing cavity with Nd:YVO<sub>4</sub> as a gain medium: It did not interrupt laser oscillation.

Currently well-aligned anisotropic laser ceramics can be produced by only the orientation control by slip-casting under the magnetic field, therefore our methods should be the solution for appreciating advantages of anisotropic laser gain media and ceramic gain media, simultaneously.

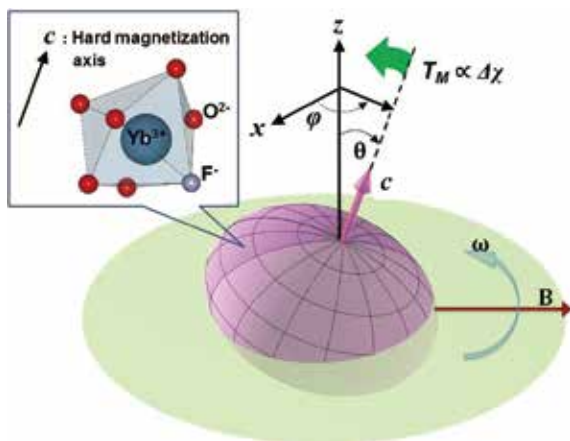


**Figure 2.** Schematic diagram for the spheroidal of magnetic energy of the processed particle under the rotating magnetic field. This particle is made of FAP doped with Yb<sup>3+</sup>, of which main crystal axis is hard magnetization axis.

## 2. Compact Megawatt Peak Power 266 nm Laser at 1 kHz

Compact and stable megawatt peak power 266 nm laser at 1 kHz from sub-nanosecond passively Q-switched laser was demonstrated. In order to optimize thermal management and obtain stable UV laser operation at high repetition rate 1 kHz, we put forward to increase pump efficiency by employing higher pump power laser diode while maintaining the low

depolarization ratio by fixing specific angle between <110>-cut Cr:YAG and <100>-cut composite YAG/Nd:YAG crystal. Megawatt peak power UV laser (266 nm) at 1 kHz is important for developing Time-of-Flight Mass Spectrometer with the technology of Single Photon Ionization (SPI).

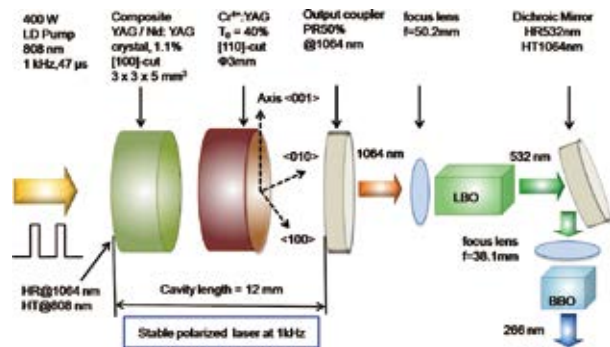


**Figure 3.** Schematic diagram of 266 nm laser at 1 kHz.

## 3. Optical Parametric Mid-Infrared Generation Pumped by Sub-Nanosecond Microchip Laser

Single-pass Mid-infrared optical-parametric generation (OPG) pumped by microchip laser with sub-nanosecond duration was demonstrated. Effective single-pass OPG with 1 mJ output energy using conventional PPMgLN could be realized. Broadband single-pass OPG could be also realized using chirped PPMgLN.

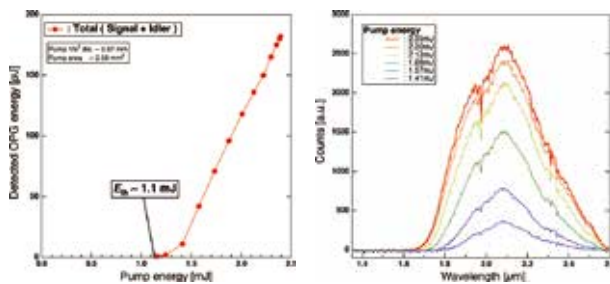


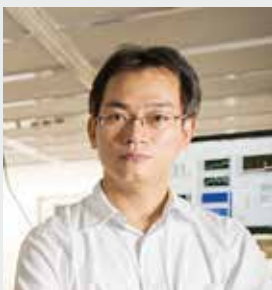
**Figure 4.** (a) OPG output on input pump energy, (b) OPG spectrum on various pumping energy, using a chirped PPMgLN.

## References

- 1) Y. Sato and T. Taira, *Opt. Mater. Express* **4**, 2006–2015 (2014).
- 2) T. Taira, A. Kausas and L. Zheng, *Nonlinear Optics (NLO2015)*, NTu3B.2 (July 26–31, 2015).
- 3) H. Ishizuki and T. Taira, *The 62<sup>nd</sup> JSAP Spring meeting 2015*, 13a-A13-3 (Mar. 11–14, 2015).

# Ultrafast Laser Science

## Laser Research Center for Molecular Science Division of Advanced Laser Development



**FUJI, Takao**  
Associate Professor  
[fuji@ims.ac.jp]

### Education

1994 B.S. University of Tsukuba  
1999 Ph.D. University of Tsukuba

### Professional Employment

1999 Assistant Professor, The University of Tokyo  
2002 JSPS Postdoctoral Fellowship for Research Abroad, Vienna University of Technology (–2004)  
2004 Guest Researcher, Max-Planck-Institute of Quantum Optics  
2006 Research Scientist, RIKEN  
2008 Senior Scientist, RIKEN  
2010 Associate Professor, Institute for Molecular Science  
Associate Professor, The Graduate University for Advanced Studies

### Awards

1999 Encouragement Award, The Optical Society of Japan  
2008 Kondo Award, Osaka University  
2015 Laser Research Development Award, the Laser Society of Japan

### Member

Assistant Professor  
NOMURA, Yutaka  
IMS Research Assistant Professor  
SHIRAI, Hideto  
Visiting Scientist  
LIVACHE, Clement\*  
Secretary  
MASUDA, Michiko

**Keywords** Ultrafast Science, Laser Physics, Nonlinear Optics

Light is very common in daily life, on the other hand, light has many interesting physical properties, for example, constancy of velocity, wave-particle duality, *etc.* The study of light is still important in modern physics.

Light is electro-magnetic field, same as radio wave, however, the measurement of the waveform of light is not easy task even in the 21<sup>st</sup> century. The difficulty comes from the extremely fast oscillation of the light wave. The oscillation frequency of light wave is the order of hundred terahertz (THz =  $10^{12}$  Hz), in other words, the oscillation period of light wave is the order of femtosecond (fs =  $10^{-15}$  s).

In 2013, we have developed a new method for the measurement of light wave. It is called FROG-CEP, frequency-resolved optical gating capable of carrier-envelope determination. Our method does not need attosecond pulses, even self-referencing is possible. The electric field oscillation of infrared light with the period of several femtoseconds were clearly measured with the method as is shown in Figure 1.

Currently, amplitude modulation and phase modulation are common encoding techniques in optical communication. If we can encode information in the shape of the light wave itself,

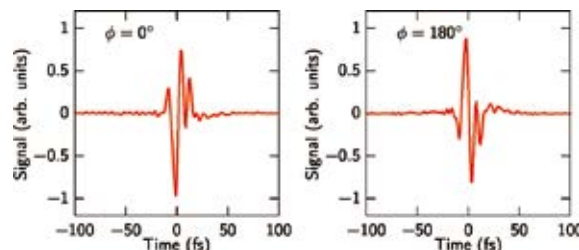


**Figure 1.** Infrared light waveforms measured with FROG-CEP. The phase difference between the two infrared pulses was clearly measured.

the communication speed becomes 3 orders of magnitude faster. We believe that our method, FROG-CEP, becomes very important to realize such communication technology.

Other than FROG-CEP, ultrabroadband mid-infrared continuum generation through filamentation and single-shot detection of ultrabroadband mid-infrared spectra has been realized in our laboratory. We are developing such cutting edge technologies for ultrafast laser science.

### Selected Publications

- T. Fuji and Y. Nomura, "Generation of Phase-Stable Sub-Cycle Mid-Infrared Pulses from Filamentation in Nitrogen," *Appl. Sci.* **3**, 122–138 (2013).
- Y. Nomura, H. Shirai and T. Fuji, "Frequency-Resolved Optical Gating Capable of Carrier-Envelope Phase Determination," *Nat. Commun.* **4**, 2820 (11 pages) (2013).
- H. Shirai, C. Duchesne, Y. Furutani and T. Fuji, "Attenuated Total Reflectance Spectroscopy with Chirped-Pulse Upconversion," *Opt. Express* **22**, 29611–29616 (2014).
- Y. Nomura M. Nishio, S. Kawato and T. Fuji, "Development of Ultrafast Laser Oscillators Based on Thulium-Doped ZBLAN Fibers," *IEEE J. Sel. Top. Quantum Electron.* **21**, 0900107 (7 pages) (2015).
- Y. Nomura, Y.-T. Wang, A. Yabushita, C.-W. Luo and T. Fuji, "Controlling the Carrier-Envelope Phase of Single-Cycle Mid-Infrared Pulses with Two-Color Filamentation," *Opt. Lett.* **40**, 423–426 (2015).
- T. Fuji, Y. Nomura and H. Shirai, "Generation and Characterization of Phase-Stable Sub-Single-Cycle Pulses at  $3000\text{ cm}^{-1}$ ," *IEEE J. Sel. Top. Quantum Electron.* **21**, 8700612 (12 pages) (2015).

## 1. Attenuated Total Reflectance Spectroscopy with Chirped-Pulse Upconversion<sup>1,2)</sup>

Attenuated total reflectance Fourier-transform infrared spectroscopy (ATR-FTIR) is a powerful tool to study liquid or solid samples in various scientific and industrial fields. However, the time resolution of the Fourier-transform infrared spectroscopy (FTIR) with the rapid scan mode is limited by the speed of the FTIR device which needs time (at least several milliseconds) for scanning the delay of the interferometer.

Chirped-pulse upconversion<sup>1)</sup> is a noteworthy method to improve the time resolution of IR spectroscopy. In this method, an infrared beam is upconverted into a visible beam and the spectrum is measured with a high performance visible dispersive spectrometer. Here, we report attenuated total reflectance (ATR) spectroscopy connected with chirped-pulse upconversion. Single-shot IR absorption spectrum measurement of liquids from 200 to 5500  $\text{cm}^{-1}$  has been realized.<sup>2)</sup>

We performed a proof-of-principle experiment by continuously recording IR spectra while exchanging the liquid on the ATR prism from water to acetone and vice versa. The rapid solution exchanging system is a useful tool to study some biological samples at advanced time-resolved ATR-FTIR spectroscopy. It is possible to monitor the IR spectrum in real-time with initiating some chemical reactions by exchanging the solutions on the ATR crystal by using two pneumatic drive pump systems, which are generally used in a stopped flow system.

We show the absorption change at 1230 and 3400  $\text{cm}^{-1}$  in the time domain in Figure 2. At 169 and 422 ms only water and acetone, respectively, should be on the ATR prism. 182 ms is the timing at which the exchange occurs. It is clear that the exchange is finished within 10 ms.

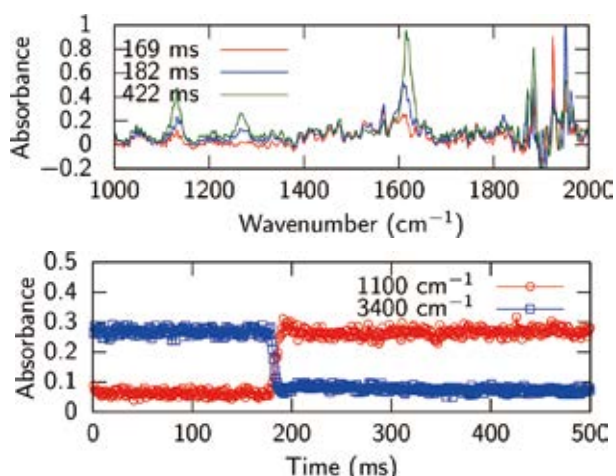


**Figure 2.** Measured dynamics of exchange of liquids with the rapid solution-exchange ATR-CPU system. Upper figure: Absorption spectra at each timing. Lower figure: Absorption change at each frequency.

## 2. Controlling the Carrier-Envelope Phase of Single-Cycle Mid-Infrared Pulses with Two-Color Filamentation<sup>5)</sup>

The rapid development of ultrafast laser technology in the last decade has made it possible to study dynamics of electrons in atoms and molecules on attosecond time scale. One of the most famous schemes of attosecond time-resolved spectroscopy is based on attosecond streaking, which is direct waveform measurement of few-cycle electric field using attosecond pulses. In this method, both an extreme ultraviolet attosecond pulse and the target pulse are focused into a noble gas, and measurement of the kinetic energy of the photoelectrons produced by the extreme ultraviolet pulse reflects the vector potential induced by the target field.

In 2013, Fuji *et al.* has developed a new waveform measurement scheme, frequency-resolved optical gating capable of carrier-envelope phase determination (FROG-CEP).<sup>3,4)</sup> The concept is based on a combination of frequency-resolved optical gating (FROG) and electro-optic sampling (EOS), which enables us to determine not only the intensity and (relative) phase profile but also carrier-envelope phase (CEP) at the same time. There are a lot of advantages of the new scheme, such as all-optical method, variety of nonlinear interactions, and possibility of single-shot measurement.

We applied the method for investigation of the phase of the single-cycle pulses generated through multi-color laser filamentation.<sup>5-7)</sup> We have experimentally found that the CEP variation depends on the frequency of the generated pulses. The phase of high frequency components of the generated pulses continuously and linearly changes with the relative phase between the two-color input pulses, on the other hand, the phase of the low frequency components takes only two discrete values. We have numerically simulated the CEP variation based on the two different models, four-wave mixing and photocurrent. Eventually, both the models are consistent with the experimental results.<sup>8)</sup>

### References

- 1) Y. Nomura, Y.-T. Wang, T. Kozai, H. Shirai, A. Yabushita, C.-W. Luo, S. Nakanishi and T. Fuji, *Opt. Express* **21**, 18249–18254 (2013).
- 2) H. Shirai, C. Duchesne, Y. Furutani and T. Fuji, *Opt. Express* **22**, 29611–29616 (2014).
- 3) Y. Nomura, H. Shirai and T. Fuji, *Nat. Commun.* **4**, 2820 (2013).
- 4) H. Shirai, Y. Nomura and T. Fuji, *IEEE Photonics J.* **6**, 3300212 (2014).
- 5) Y. Nomura, H. Shirai, K. Ishii, N. Tsurumachi, A. A. Voronin, A. M. Zheltikov and T. Fuji, *Opt. Express* **20**, 24741–24747 (2012).
- 6) T. Fuji and Y. Nomura, *Appl. Sci.* **3**, 122–138 (2013).
- 7) T. Fuji, Y. Nomura and H. Shirai, *IEEE J. Quantum Electron.* **21**, 8700612 (2015).
- 8) Y. Nomura, Y.-T. Wang, A. Yabushita, C.-W. Luo and T. Fuji, *Opt. Lett.* **40**, 423–426 (2015).

### Award

FUJI, Takao; NOMURA, Yutaka; SHIRAI, Hideto; Laser Research Development Award, the Laser Society of Japan (2015).

# Dissociative Photoionization Studies of Fullerenes and Carbon Nanotubes and Their Application to Dye-Sensitized Solar Cells

Department of Photo-Molecular Science  
Division of Photo-Molecular Science III



KATAYANAGI, Hideki  
Assistant Professor

We have studied the mechanisms and kinetics of dissociative photoionization of fullerenes by means of the velocity map imaging spectroscopy. We now intend to apply the above gas phase spectroscopy to functional materials such as carbon nanotubes (CNTs). Additionally we apply the CNT and fullerene derivatives to a catalytic counter electrode (CE) in dye-sensitized solar cells (DSSCs).

## 1. Mass Resolved Velocity Map Imaging of Doubly Charged Photofragments from C<sub>60</sub> and C<sub>70</sub>

We have obtained 2D velocity images of the fragments from C<sub>60</sub><sup>1+</sup> and C<sub>70</sub> with improved resolution. The 2D velocity images of fragments were found to be convolutions of isotropic center-of-mass velocity acquired by the C<sub>2</sub> emission and anisotropic velocity of C<sub>60</sub> in the parent molecular beam.

## 2. Gas Phase Spectroscopy of CNTs

We built a vacuum apparatus for the gas phase spectroscopy of CNTs. With the apparatus we will perform experiments using the fullerenes and then improve the chamber to achieve experiments using CNTs.

## 3. Development of the Counter Electrodes Using CNTs and Fullerene Derivatives and Evaluation of Their Feasibility for DSSCs

To improve efficiency, lifetime and cost of the DSSC, materials to make the CE need to be reconsidered. We prepared the CEs using commercial CNT aqueous dispersions and succeeded in fabricating DSSC cells which showed reasonable efficiency. We have started to make CEs using sulfonated fullerenes. We produced Langmuir-Blodgett (LB) films of the sulfonated fullerenes on glass substrates. We will evaluate the feasibility of the LB films for the DSSCs.

### Reference

1) H. Katayanagi and K. Mitsuke, *Bull. Chem. Soc. Jpn.* **88**, 857–861 (2015).

# Soft X-Ray Spectro-Microscopy for *In-Situ* Chemical Imaging

UVSOR Facility  
Division of Beam Physics and Diagnostics Research



OHIGASHI, Takuji  
Assistant Professor

A scanning X-ray transmission microscopy (STXM) is a powerful tool<sup>1)</sup> for *in-situ* chemical imaging. In the present work, we have developed a humidity control sample cell for the chemical and morphological analysis of a fuel cell under the working condition, such as high temperature and high humidity. The sample cell is consisted of two silicon nitride windows with 100 nm thickness and a chamber. A small sensor (SHT7x, Sensirion AG) is placed near the sample in the chamber to monitor the humidity and the temperature. The chamber is equipped with three gas ports and the humidity of the sample can be controlled by flowing dry or humid helium gas in the sample cell.

With changing the humidity inside the sample cell from 8 to 83% at room temperature, a thin section (thickness of 100 nm) of the fuel cell has been observed. The optical density images of a porous polymer electrode of the fuel cell are

shown in Figure 1. These images were acquired by using the photon energy at 285.5 eV and the dwell time per a pixel was 10 ms. In a high humidity condition, the area of the polymers (shown as white color) increases and the voids (shown in dark color) decreases. This result implies that the porous polymers are swelled by absorbing the water vapor.

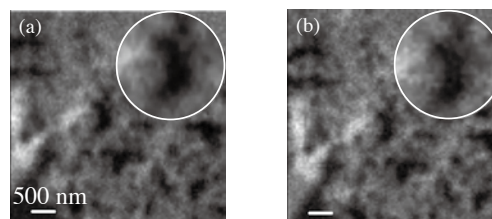


**Figure 1.** OD images of the electrode at the humidity of (a) 8% and (b) 83%. Inset images are blowup of the same area.

### Reference

1) T. Ohigashi, H. Arai, T. Araki, N. Kondo, E. Shigemasa, A. Ito, N. Kosugi and M. Katoh, *J. Phys.: Conf. Ser.* **463**, 012006 (2013).

## Visiting Professors



Visiting Professor  
**IMURA, Kohei** (*from Waseda University*)

### Development of Advanced Super-Resolution Microscopy and Their Application to Nanomaterials

Near-field optical microscopy overcomes the diffraction limit of light and achieves a nanometer spatial resolution. We have developed various near-field spectroscopic methods such as transmission, non-linear excitation, ultrafast time-resolved imaging, and utilized them to study optical properties of nanomaterials.

We have been extending these studies into two directions: (1) development of advanced super-resolution microscopy based on various microscopes, and (2) spatio-temporal control of elementary excitations and photochemical reactions using nanomaterials. We have developed near-field reflection microscope and cathodoluminescence electron microscope. The microscopy enables to visualize spatial distribution of eigen modes excited in nanomaterials on transparent and non-transparent substrate with a wide spectral range. Recently, we found that optical field distribution excited in the nanomaterials varies with amplitudes and phases of ultrashort pulses illuminated. This indicates that coherent control of elementary excitations and photochemical reactions are feasible in space and time resolved manner. We are currently exploring novel photochemical reaction schemes assisted with designed optical fields.



Visiting Associate Professor  
**YAMADA, Toyo Kazu** (*from Chiba University*)

### Dimensional Dependence of Organic Molecular Electronic States

Scanning tunneling microscopy (STM) has been used to visualize material topology with an atomic scale. In last 15 years I have developed STM to visualize not only atomic structures of materials but also electronic, spin, and quantum structures combined with spectroscopy techniques. 1-nm-size nano-materials, such as nano-magnets, single atoms, single molecules, and graphene nano-ribbons have been studied for

realizing new nano-electronic devices with low cost, low power consumption, and high performance. In 2015, we glow two-dimensional molecular networks on an atomically-flat noble metal substrate. The surface structures are directly observed by STM. Subsequently, a magnetic metal is deposited on the network, then we can glow new two-dimensional magnetic nano-dot arrays. We study electronic and magnetic structures of the magnetic array by means of STM spectroscopy and the photoemission spectroscopy. All experiments are performed in ultra-high vacuum. We try to control electronic/quantum spin structures of magnetic arrays by using two-dimensional molecular networks.



Visiting Associate Professor  
**HIRAHARA, Toru** (*from Tokyo Institute of Technology*)

### Spin-Split States at the Surface/Interface of Nonmagnetic Ultrathin Films

Recently there has been growing interest in utilizing the spin degree of freedom in electronic devices, the so-called spintronics. The conventional way is to use magnetic materials and manipulate the spin using a magnetic field. However, it is sometimes troublesome to apply a magnetic field to nano-scale materials and it is much easier to control the spin properties of materials using an electric field. By making use of the

Rashba effect in which electrons become spin polarized in k-space due to spin-orbit coupling effects at the surface, such manipulation of electron spin with an electric field becomes possible, i.e., a spin field effect transistor can be realized in such materials. We plan to develop a high-resolution spin- and angle- resolved photoemission spectroscopy measurement system equipped with in situ sample preparation facilities at BL-5U and characterize the novel spin property at the Rashba-split surface/interface states of nonmagnetic ultrathin films.

# RESEARCH ACTIVITIES

---

